

E.S. Fortune
G.J. Rose

Department of Biology, University of Utah,
Salt Lake City, Utah, USA

Temporal Filtering Properties of Ampullary Electrosensory Neurons in the Torus semicircularis of *Eigenmannia*: Evolutionary and Computational Implications

.....
Key Words

Whole-cell patch
Frequency filtering
Spines
Evolution of behavior

.....
Abstract

Weakly electric fish have parallel electrosensory systems, the phylogenetically older ampullary system and the novel tuberous system. The tuberous system is an adaptation related to the evolution of active electrolocation. To examine the evolutionary relationship of the ampullary and tuberous systems, the temporal filtering properties of ampullary neurons in the dorsal torus semicircularis of *Eigenmannia* were studied. 'Whole-cell' recordings were made in vivo using patch-type pipettes. The responses of 19 neurons to sinusoidal electric signals (<40 Hz) were recorded and the anatomy of these neurons demonstrated by injection of biocytin. All eight low-pass ampullary neurons had broad, relatively smooth post-synaptic potentials (psps) that at low frequencies nicely reflected the sinusoidal stimuli. These neurons had somata of 10-14 μm diameter and thick, spiny dendrites. Eight high-pass neurons were recorded, representing three physiological classes. The first class (3 neurons) had psps that roughly followed the sinusoidal time course of the stimulus; the psp morphology was similar to low-pass neurons. The second class had many small, fast, individual psps; their rate of occurrence varied with the stimulus. Finally, four neurons showed psps that were of constant width across stimulus frequencies. All three classes of high-pass neurons had small somata (8-10 μm diameter) with thin dendrites and either few or no spines. Some of these neurons had large varicosities on the dendrites. Three neurons had band-pass filtering properties: neurons that showed strong band-pass properties were morphologically similar to low-pass neurons. Comparisons of the temporal filtering, shapes of post-synaptic potentials, and anatomy of ampullary and tuberous neurons in the torus suggest that the circuitry for tuberous processing in the torus may have evolved as an elaboration or duplication of the ampullary system. The mechanisms underlying the low-pass filtering characteristics of tuberous neurons therefore appear to have predated the evolution of the tuberous system and to have served as a pre-adaptation for the evolution of the jamming avoidance response. In addition, these data support the hypothesis that spine density influences the temporal filtering properties of neurons.

.....

Introduction

The evolution of behavior requires that complex networks of sensory and motor neurons be adapted to solve novel computational problems. How neural circuits are modified for new behaviors is a major problem in evolutionary neurobiology. One possibility is that new circuits may evolve as elaborations or duplications of plesiomorphic circuits. *Eigenmannia*, a genus of South American fishes, produce and detect weak electric fields, which are used in a variety of novel behaviors including electrolocation, jamming avoidance, and social communication [see Heiligenberg, 1991; Bullock and Heiligenberg, 1986]. *Eigenmannia* has two parallel electrosensory systems, the phylogenetically older ampullary system and the novel tuberous system [Zakon, 1986]. The neural circuitry of the tuberous system, which is required for active electrolocation and jamming avoidance, may have been derived from the plesiomorphic circuitry of the ampullary system. Alternatively, features of the tuberous system may have evolved independently for the control of jamming avoidance. We have investigated temporal processing in the ampullary system of *Eigenmannia* to determine the evolutionary relationship between the ampullary and tuberous systems.

Ampullary electroreceptors are broadly sensitive to low frequency electric signals, typically below 50 Hz, and are found in many species of aquatic vertebrates, including most non-teleosts, four orders of teleosts, and some urodeles [for review see Zakon, 1986; Roth and Schlegel, 1988]. Fossil evidence indicates that ampullary-like receptors may also have been present in some Devonian fishes [Thomson, 1977]. These and other data suggest that ampullary-like receptors are a primitive character of vertebrates [Bodznick and Northcutt, 1981]. In contrast, tuberous electroreceptors are present only in two groups of distantly related teleosts. These two groups, the South American gymnotiforms and the African mormyriiforms, have independently evolved electrogenic organs that produce weak electric fields surrounding the fish [Hopkins, 1976, 1983]. Tuberous receptors are generally tuned near the frequency of an individual's electric organ discharge (EOD).

Local modulations of the amplitude and phase of a fish's EOD can result from its relative movement with respect to objects in its environment. These modulations can be detected by the tuberous system and used by the fish to characterize and localize these objects [Heiligenberg, 1973; Bastian, 1986; Rose et al., 1987]. Electrolocation can be impaired in *Eigenmannia* by introducing an EOD from another fish; the interaction between the EODs of the two fish also causes fluctuations in the amplitude and phase of the

signals detected by the tuberous system [Matsubara and Heiligenberg, 1978]. Differences in EOD frequencies (the 'beat rate') of between 3 to 8 Hz are most detrimental to electrolocation, whereas beat rates above 20 Hz do not impair electrolocation [Bullock et al., 1972; Heiligenberg, 1973]. To minimize this interference, *Eigenmannia* reflexively adjusts its EOD frequency to increase the difference in EOD frequencies of the two fish; this behavior is known as the jamming avoidance response (JAR).

Several classes of electrosensory neurons in the torus have complex properties that likely contribute to the detection of behavioral conditions that elicit the JAR [see Heiligenberg, 1991]. These include tuberous neurons that respond best to beat rates of 2–6 Hz [Partridge et al., 1981; Rose and Heiligenberg, 1986]. However, such neurons may have more generalized functions, as moving stimuli can generate modulations at these frequencies [Bastian, 1986; Rose et al., 1987]. Also, the primitive genus *Sternopygus*, which does not have a JAR, nonetheless has toral neurons similar to those identified in *Eigenmannia* as 'detectors' for the JAR [Rose et al., 1987]. Thus, temporal processing in the torus may have evolved in the context of electrolocation and served as a pre-adaptation for the JAR.

In this study we explored the possibility that the ampullary and tuberous systems have similar temporal filtering properties. Our goal was to identify and compare the temporal filtering properties, mechanisms, and anatomy of ampullary neurons with those for tuberous neurons described in previous reports. Whole-cell recordings with patch-type pipettes ('whole-cell patch') were made in the torus of the weakly electric fish *Eigenmannia*, in vivo. This technique has several advantages. First, both extracellular and intracellular recordings from individual neurons can be obtained. Second, neurons can be thoroughly labeled by injection of biocytin. Lastly, this technique permits recordings from classes of small neurons that are rarely achieved using standard sharp electrodes. This report describes the temporal filtering, fine temporal structure of post-synaptic potentials (psps), and morphology of ampullary neurons in the torus. We found that neurons with low-pass filtering characteristics are spiny, whereas high-pass neurons have few or no spines. The classes of ampullary neurons are similar both in physiology and anatomy to tuberous neurons in the torus.

Materials and Methods

Experimental procedures were similar to those used in earlier investigations of the torus [Heiligenberg and Rose, 1985; Rose and Call, 1992, 1993], except that all recordings were made using whole-cell

patch recording methods. The techniques used to obtain whole-cell recordings are described in detail by Rose and Fortune [1996]. Fish of the genus *Eigenmannia* were used. The fish's EOD was measured and then attenuated (~1,000 fold) by intramuscular injection of Flaxedil (4 µg/g fish). Additional injections of Flaxedil were made during the experiment as necessary to maintain the attenuation of the EOD. Animal husbandry, anesthesia, and surgical procedures were performed under guidelines established by the Society for Neuroscience.

The fish's EOD was replaced by a sinusoidal mimic (S1) which was delivered through electrodes placed at the tail and in the mouth. The amplitude and frequency of the S1 was adjusted to approximate the fish's EOD before the injection of Flaxedil. While searching for neurons, a linear frequency sweep (2–30 Hz, 10 sec duration, 1–2 mV/cm at the fish) was added to the S1, and a third signal (S2), 4 Hz higher or lower than the S1 frequency, was either added to the S1 or delivered through one pair of an array of carbon electrodes surrounding the fish. When an ampullary neuron was isolated, the S1 was replaced with the 10 second low-frequency sweep, and the S2 was removed. In a few cases the frequency sweep was delivered through a pair of the carbon electrodes surrounding the fish.

Patch pipettes were constructed from borosilicate capillary glass (A-M systems #7052; 1 mm outer diameter, 0.58 mm inner diameter) using a Flaming-Brown type puller (Sutter Instruments, model P-97). Electrodes were pulled in three stages to resistances between 20 and 30 MΩ. Electrode tips were back-filled with 1.5% w/v biocytin (Molecular Probes, Eugene OR) in a 285 to 290 mOsmol. solution (pH 7.2) containing (values in mM) 100 potassium acetate, 2 KCl, 1 MgCl₂, 5 EGTA, 10 HEPES, 20 KOH, and 43 biocytin. Biocytin was replaced by mannitol in the solution used to fill pipette shanks. A second set of solutions had 10 mM KCl and 92 mM potassium acetate – no detectable differences were apparent between recordings with each of these solutions.

For recordings, electrodes were mounted in a plexiglass holder with a pressure port. This port allowed the application of pulses (20–60 msec) of high-pressure (40 PSI) from a Picospritzer (General Valve Corp.) or the manual application of suction or pressure from a 30 cc syringe. The electrode was advanced in 1.5 µm steps (Burleigh microdrive) through the top five layers of the torus. Responses were amplified using an electrometer (model 767, World Precision Instruments, Sarasota FL) and stored on video tape at 40 kHz with 16 bit resolution (Vetter Instruments).

A small amount of positive pressure (1–2 cc) was applied while advancing the electrode through the tissue. Neurons were detected by an abrupt increase in resistance and the appearance of spikes and/or ripples in the recording trace. Suction (2–5 cc) was applied until a seal resistance of approximately 300–400 MΩ and monophasic spikes were observed. In many instances suction did not improve the recording and resulted in obstruction of the pipette tip. In such cases, the pipette was cleared by withdrawing it several micra, applying pressure pulses and, when necessary, several nanoamps of negative current. In those cases where a stable monophasic extracellular recording was established, responses to the frequency sweeps were recorded. To improve the seal further, approximately –0.2 nA DC was applied in conjunction with slight additional suction. Further suction was avoided as it often resulted in damage to the cells. Instead, the membrane patch was ruptured by manually applying negative current (<1 nA) to the electrode while maintaining the suction.

Once psp's of at least 10 mV were seen, most neurons were then hyperpolarized such that psp's could be observed in the absence of spike generation. Increased hyperpolarization resulted in an increase in the

amplitude of psp's in all but four neurons. For these four neurons, increased hyperpolarization led to an abrupt decrease in the amplitude of the psp's, suggesting that a major component of the psp's was a voltage dependent conductance.

Frequency sweeps were presented at amplitudes from approximately 0.5 to 2.0 mV/cm, followed by other test stimuli. These stimuli included 1-sec sinewave bursts at frequencies from 5 Hz–40 Hz and square waves. If the recording was stable, the level of current injection was altered and the stimuli presented again. Neurons were then filled by applying 1–2 nA of positive DC current for 1–3 minutes.

Animals were deeply anesthetized by immersion in 2% w/v urethane between one and three hours after the first neuron was filled – up to four neurons were filled per fish. Animals were perfused transcardially with saline-heparin solution followed by 4% w/v paraformaldehyde in 0.2 M phosphate buffer (pH=7.4). The brain was removed and stored at 4 °C overnight in the paraformaldehyde solution. One-hundred micron sections were cut on a vibratome and reacted using an avidin-biotin peroxidase kit (Vector Laboratories, Burlingame MA). Sections were dehydrated, cleared in xylenes, mounted on slides, and coverslipped. Neurons were traced and their morphology analyzed with a computer three-dimensional tracing system (Eutectic Co.).

The temporal filtering profiles of neurons were determined by Fourier analysis of several 500 msec segments of the intracellular responses to frequency sweeps. Spikes, when present, were digitally removed before analysis. The peak of the power spectrum near to the stimulus frequency was used as a measure of the amplitude of stimulus-related psp's at that frequency. The filtering profiles shown in this report are from neurons that had stable recordings with less than ±1 dB variation between independent tests of a particular stimulus condition.

Results

We obtained intracellular recordings from 61 neurons, of which 27 responded to ampullary stimuli. Recordings from 19 ampullary neurons were used in this report. Eight of these neurons showed low-pass characteristics, three were band-pass, and eight were high-pass. Temporal filtering profiles (fig. 1A–C) were generated for neurons where the recording was both stable and had low access resistances resulting in maximum recorded stimulus-related psp amplitudes of at least 5 mV. Response profiles were not generated for four of the high-pass neurons because the shapes of their psp's were largely independent of stimulus frequency, and psp amplitude was non-linearly related to membrane potential (see below).

Stimulation frequencies below 10 Hz elicited the largest amplitude stimulus-related psp's from low-pass neurons (fig. 1A). Responses to high frequency stimuli (>25 Hz) were at least 7 dB below the maximum response, but there were considerable differences in the filtering characteristics between low-pass neurons. For instance, the drop in psp amplitude to 5 dB below maximum was seen at frequencies

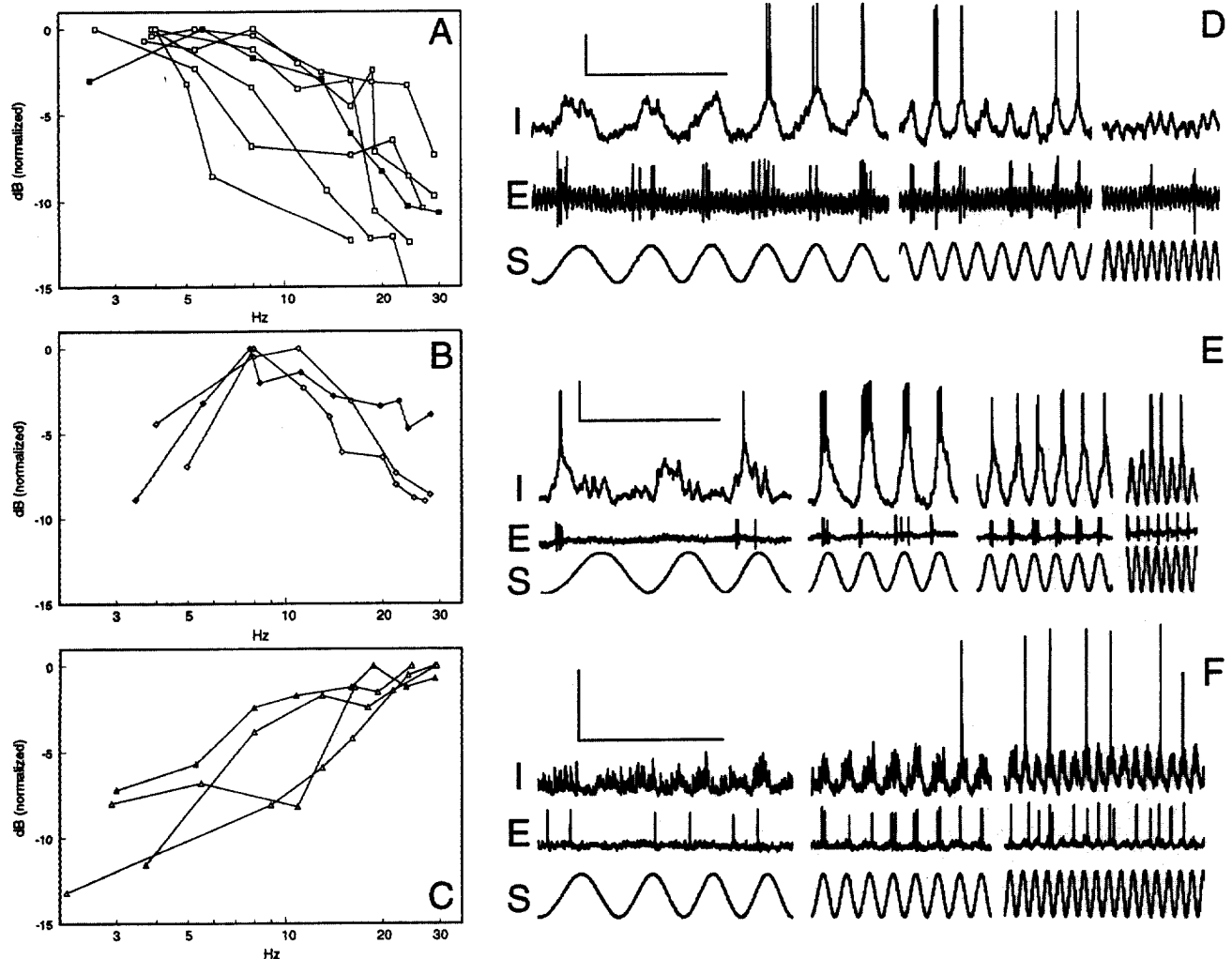


Fig. 1. Physiology of low-, band-, and high-pass ampullary neurons. **A-C** Relative amplitude of psp's as a function of frequency. These data were obtained from the intracellular responses to frequency scans (examples of which are shown in **D-F**). Values are the peak amplitude of the power spectrum obtained by Fourier analysis of short (500 msec) segments of the intracellular trace. Values for each curve were normalized relative to the maximum amplitude value for that neuron. Frequency values (X-axis) are shown on a log scale. Filled symbols in **A-C** indicate the curve for the neuron shown in **D-F**. **A** Low-pass neurons. **B** Band-pass neurons. **C** High-pass neurons. **D-F** I = Intracellular response; E = extracellular response; S = stimulus. Scale bars indicate 10 mV and 500 msec. **D** Low-pass neuron. Time-course of psp's roughly correlate to the stimulus. Three segments from the sweep are shown (3–6 Hz, 10–12 Hz, and above 25 Hz). **E** Band-pass neuron. Duration of psp's roughly correlates to the stimulus. Four segments from the sweep are shown (below 4 Hz, 7–8 Hz, between 12–13 Hz, and above 25 Hz). **F** High-pass neuron with very fast, small psp's. Three segments from the sweep are shown (below 6 Hz, 12–13 Hz, and 20–25 Hz). For more detail, see figure 2.

ranging from 6 to 24 Hz (fig. 1A). Low-pass ampullary neurons had slowly rising excitatory psp's that, in the best recordings, reached 20 mV in peak-to-peak amplitude. The psp's were broad, smooth, and relatively sinusoidal at low frequencies; at the lowest frequencies (<5 Hz) the psp's had flat tops (fig. 1D). At higher frequencies the psp's had expo-

ponential rise and fall characteristics with sharp-peaks. Unlike high-pass neurons, which were divided into three distinct classes on the basis of psp shape, all low-pass neurons had similar psp morphology.

The three band-pass neurons showed maximum amplitudes of stimulus-related psp's for stimuli from 7–11 Hz, fal-

Fig. 2. Time-expanded view of the intracellular activity of the neuron shown in figure 1F. This neuron is characterized by fast, spontaneous excitatory psp's. Scale bars indicate 2.5 mV and 50 msec.

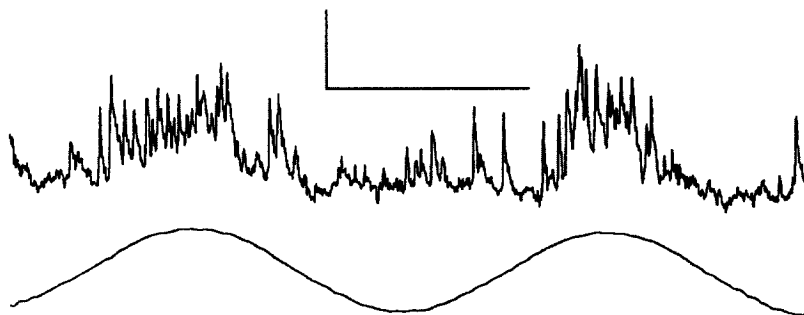
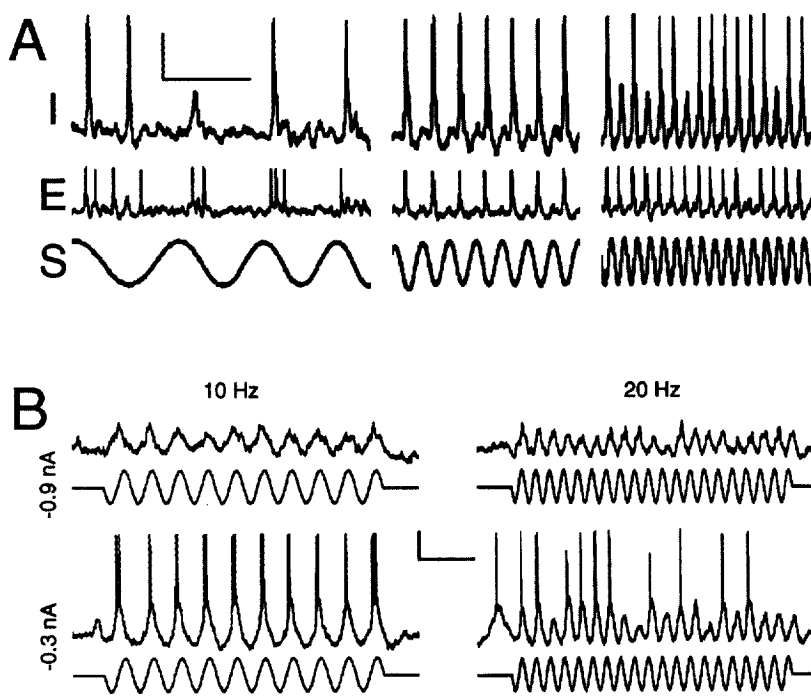


Fig. 3. High-pass ampullary neurons where psp duration does not appear to correlate to the stimulus. **A** Intracellular (I) and extracellular (E) responses to an ampullary stimulus (S). Scale bars indicate 10 mV and 250 msec. **B** Intracellular responses of a neuron with similar physiological properties at two levels of current clamp. At -0.9 nA the psp's reflect the stimulus. However, at -0.3 nA the psp's include a conductance that leads to spike generation and apparently does not vary with the stimulus. Scale bars indicate 10 mV and 200 msec.

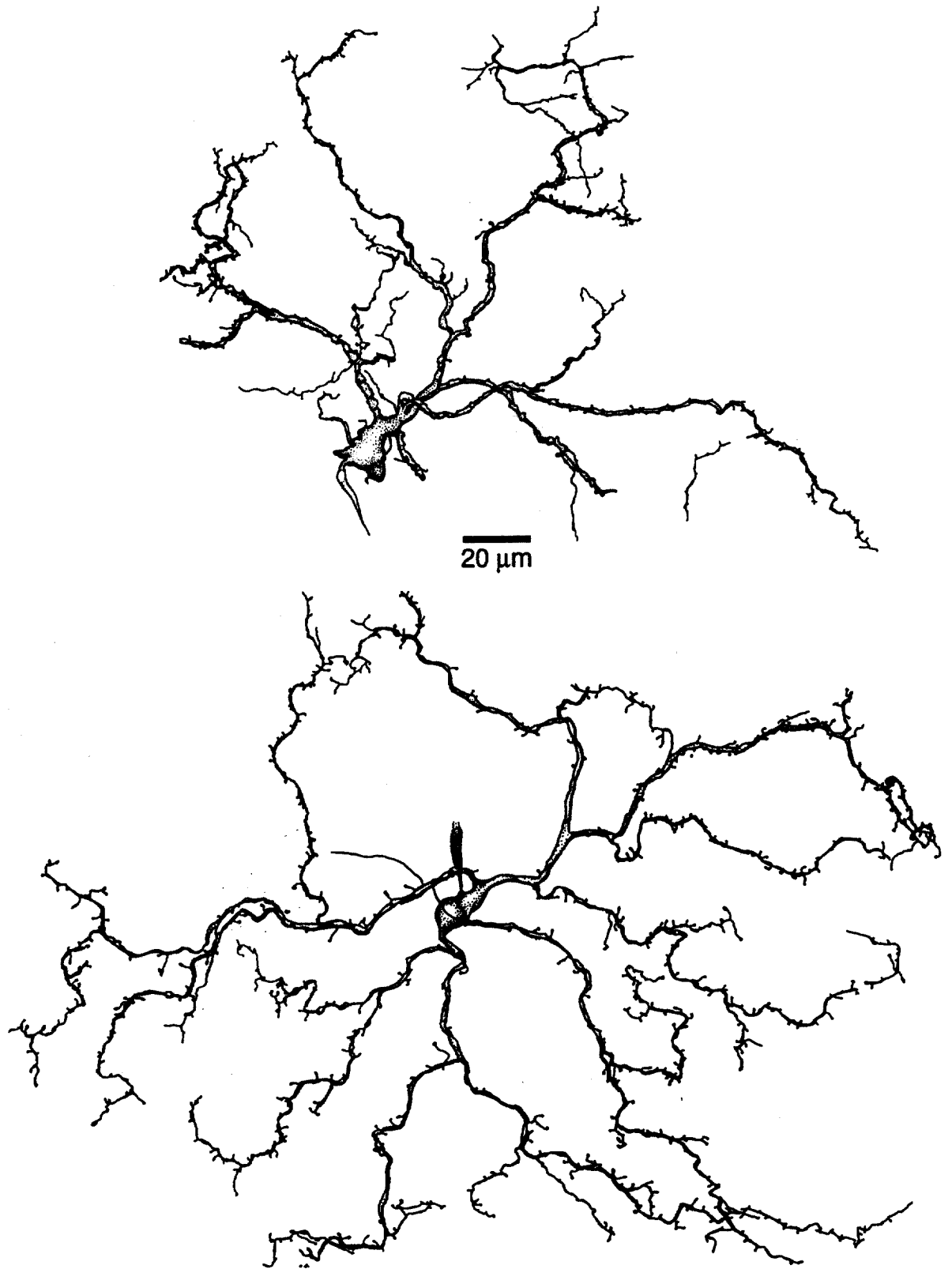


ling more than 4 dB to both lower and higher frequencies (fig. 1B). Two of these neurons had psp's with shapes that were similar to low pass neurons, except that the amplitudes of psp's elicited by the lowest frequency stimuli were greatly reduced. The stimulus-related psp's of these two neurons were smooth and relatively sinusoidal. The third band-pass neuron showed psp's that had a mixture of features from both low and high-pass neurons (fig. 1E). The width of psp's reflected the frequency of the stimulus, but individual, fast psp's were evident, especially at low frequencies.

High-pass neurons were divided into three physiological types on the basis of psp morphology. From extracellular

recordings, however, the temporal response profiles of these three classes of neurons were similar; these neurons responded best to high frequency stimuli (above 20 Hz). The first two classes of high-pass neurons showed maximum psp amplitudes to frequencies above 15 Hz (fig. 1C). The amplitude of psp's fell by more than 5 dB at stimulus frequencies of 5 Hz or below. The first class (three neurons) had psp's that roughly followed the shape of the stimulus. At low frequencies, small (<1 mV), individual, fast psp's

Fig. 4. Morphology of low-pass ampullary neurons. Physiology of the top neurons is shown in figure 1D. Electrode track is shown above the soma of the bottom neuron.



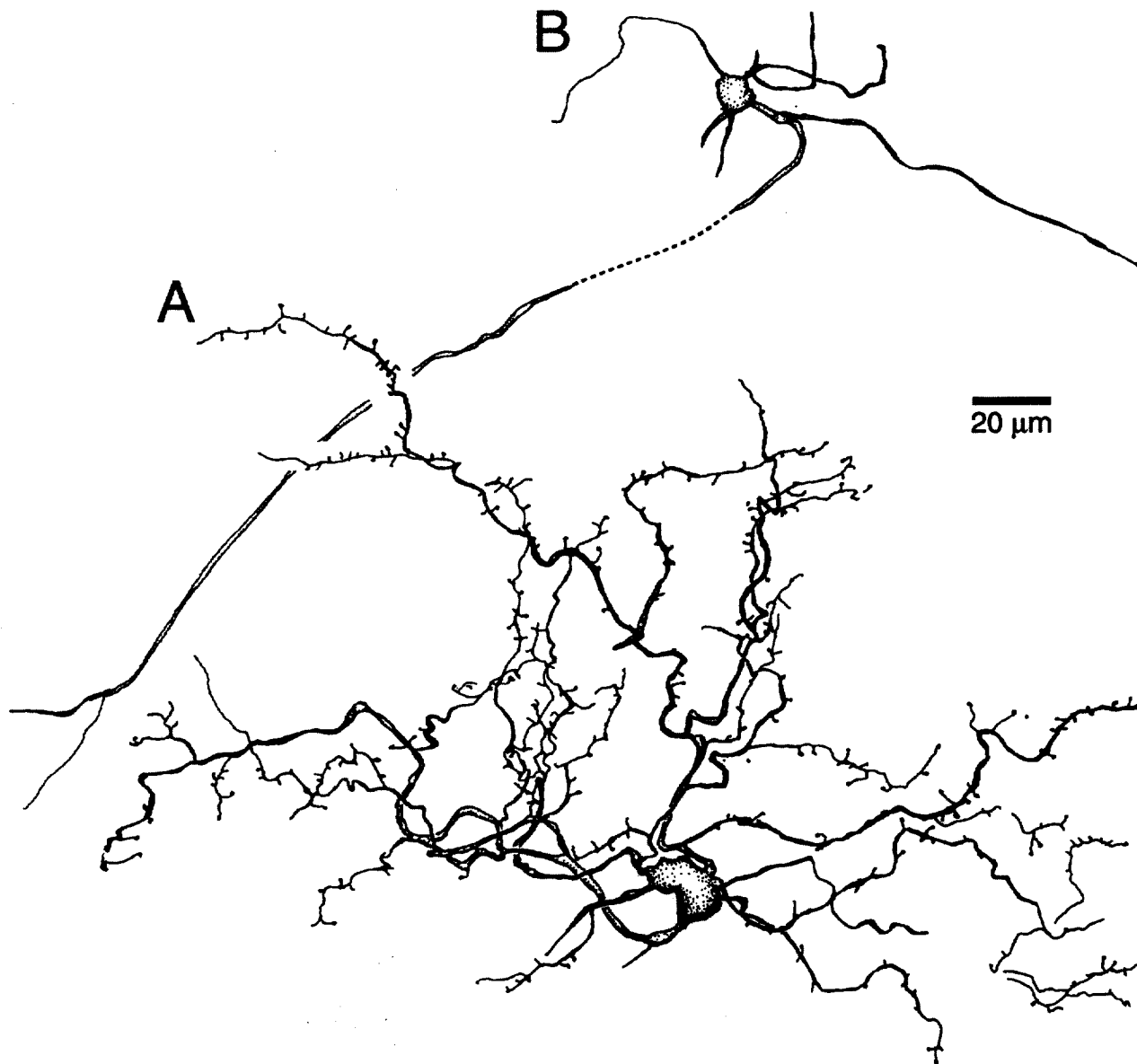


Fig. 5. Morphology of band-pass ampullary neurons. **A** Neuron with psp's that are similar in shape to low-pass neurons. **B** Neuron with psp's that are intermediate between low- and high-pass neurons. Physiology is shown in figure 1E.

were visible riding on top of quasisinusoidal fluctuations. At higher frequencies the psp's appeared smoother. In general, the shape of psp's was similar to that of the band-pass neuron shown in figure 1E, except that stimulus-related psp's had flat tops to higher (up to 18 Hz) frequencies, and the amplitude of the psp's did not decrease at the highest frequencies.

The second class had many small, fast, individual psp's that occurred spontaneously and in response to the stimulus

(fig. 1F). We recorded only one example of this class of neuron, but the physiology is similar to that of a class of tuberous neurons shown previously [see fig. 8 of Rose and Call, 1993] and encountered in the course of this study. The rise-times of spontaneous psp's were very fast; the largest spontaneous psp's (>2.5 mV) had an average rise time of 480 μ s ($n=17$, $s=6.8$), and the smallest (1–1.5 mV) had an average of 270 μ s ($n=11$, $s=5.0$). Stimulus-related psp's showed small (<5 mV) quasisinusoidal fluctuations with

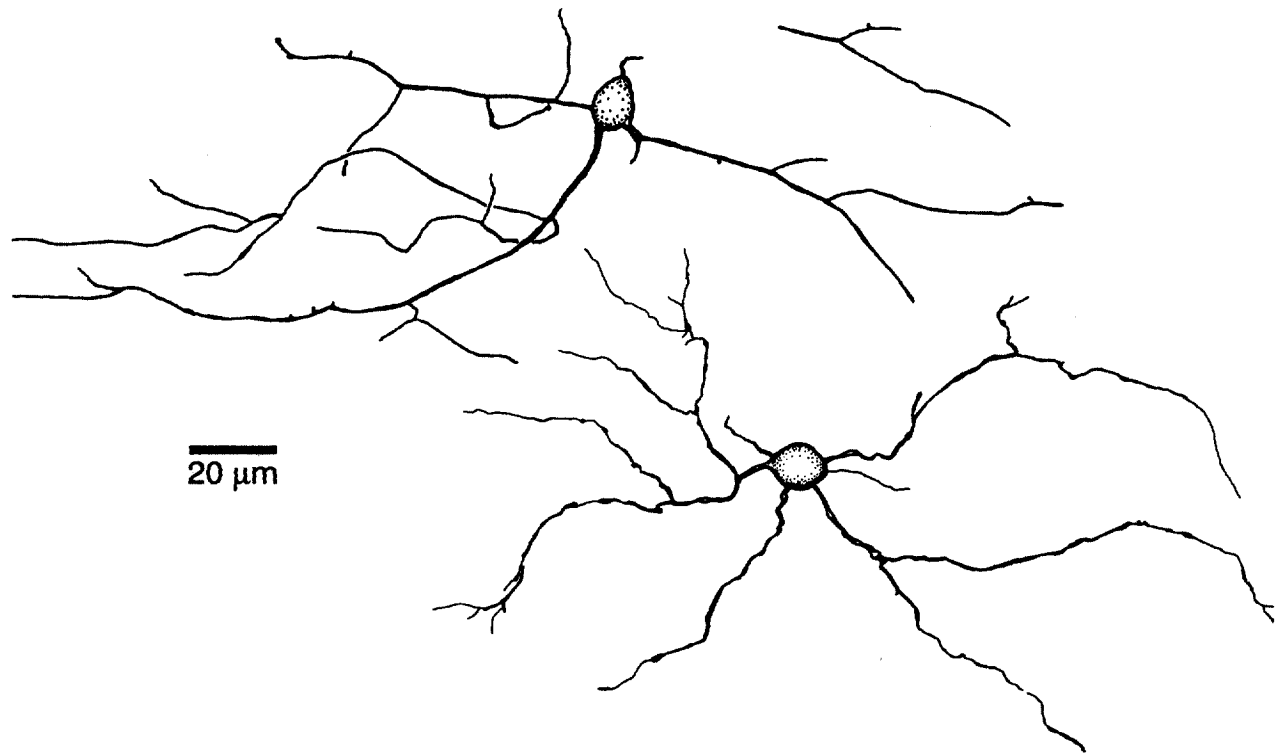


Fig. 6. Morphology of high-pass ampullary neurons. Physiology of bottom neuron is shown in figure 1F.

numerous fast psp, similar to the spontaneous psp, riding on top at all stimulus frequencies (fig. 2). At low stimulus frequencies (<5 Hz), only fast psp were observed, suggesting that baseline fluctuations at high stimulus frequencies, especially above 15 Hz, resulted from temporal summation of many individual fast conductances.

Finally, there were four neurons where the psp width did not vary with stimulus frequency (fig. 3A). When little or no hyperpolarizing current was applied, psp duration at half of the maximum amplitude for these neurons was almost constant across stimulus frequencies (at 30 Hz, $X=10.0$ ms, $n=12$, $s=0.57$; at 20 Hz, $X=11.3$ ms, $n=11$, $s=0.97$; at 10 Hz, $X=11.6$ ms, $n=10$, $s=0.74$). With increased current injection, to levels where few or no spikes were elicited, the positive inflections of these psp were eliminated, and their psp amplitude decreased (fig. 2B). Thus, the rapid constant-width psp were not necessarily a result of highly synchronized inputs, but rather of large, voltage-dependent conductances. Attenuation of these conductances by hyperpolarization revealed an underlying low amplitude psp that varied in duration with the stimulus frequency (fig. 3B).

Anatomy

Low-pass neurons had large somata (10–14 μm diameter) with proximally thick (>1 μm diameter), spiny dendrites (fig. 4). These neurons were all located in lamina IV and correspond to Golgi-labeled type b (pyramidal) neurons [Carr and Maler, 1985]. Many spines on proximal portions of dendrites appeared to be shorter and broader than spines located on more distal portions of dendrites. Distally located spines often had a thin stem with a broad head. These neurons had a plate-like distribution of dendrites oriented in the transverse plane.

Two of the three band-pass neurons were well-labeled. One of these two had psp that were similar to low-pass neurons. This neuron was a spiny pyramidal cell in lamina IV and was morphologically indistinguishable from the group of low-pass neurons (fig. 5A). The second band-pass neuron, the physiology of which was intermediate between that of low-pass and that of high-pass neurons, had few spines with medium-thick (~ 1 μm diameter) dendrites (fig. 5B). This neuron corresponds to Golgi-labeled type c neurons of lamina IV [Carr and Maler, 1985].

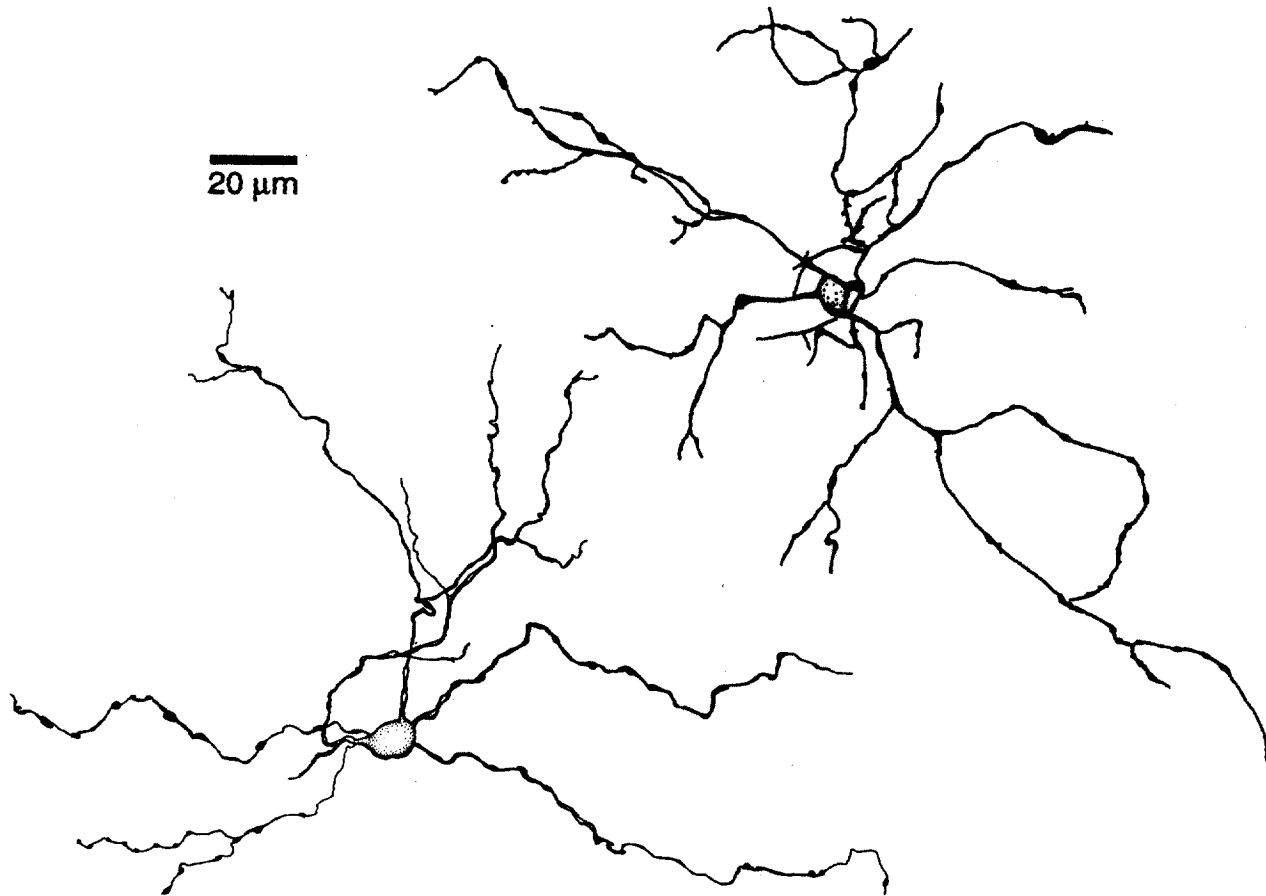


Fig. 7. Morphology of high-pass ampullary neurons with psp durations that were relatively constant across frequencies. Physiology of top neuron is shown in figure 3B.

High-pass neurons had smaller somata (8–10 μm diameter) with thin dendrites (fig. 6). These neurons had varicosities distributed along their thin ($<1 \mu\text{m}$ diameter) dendrites; such varicosities were not seen on low-pass neurons. Some neurons had a sparse distribution of spines. Neurons that showed active conductances were morphologically similar to other high-pass neurons (fig. 7). These neurons were found exclusively in laminae III and V. Quantitative morphological analysis of three well-filled examples of low-pass neurons and high-pass neurons demonstrated that low-pass neurons had more spines (low-pass $X=827$ spines, $n=3$, $s=352$; high-pass $X=66$ spines, $n=3$, $s=33$), and a greater spine density (low-pass $X=0.192$ spines/ μm^2 , $n=3$, $s=0.054$; high-pass $X=0.042$ spines/ μm^2 , $n=3$, $s=0.009$) than high-pass neurons.

Discussion

We have described the physiology and anatomy of ampullary neurons in layers III through V of the torus semicircularis of *Eigenmannia*. These neurons had low-pass, band-pass, or high-pass temporal filtering characteristics. We found that neurons with smooth stimulus-related psp, which included all low-pass and some band-pass neurons, had high spine densities, whereas all high-pass neurons, regardless of the characteristics of their psp, had low spine densities with dendritic varicosities. Thus, spine density is positively correlated with temporal filtering. The temporal filtering properties of these neurons and the shapes of their psp are similar to those seen in tuberosus neurons in the torus.

The recordings in this report were made using 'whole-cell' recording methods. This technique has two major ad-

vantages over standard intracellular recordings with sharp electrodes. First, both extracellular and intracellular recordings can be obtained from single neurons. Comparison of the extra- and intracellular recordings is a powerful control which establishes that creating an opening in the cell does not significantly affect its physiology. Second, we obtained recordings from many small neurons; such recordings are rare when using standard sharp electrodes to obtain intracellular recordings [G.J. Rose, unpubl. observ.]. Previous studies of the tuberous system show recordings primarily from large, low-pass neurons [Rose and Call, 1993]. In contrast, we encountered equal numbers of low- and high-pass neurons in both ampullary (presented above) and tuberous modalities [not shown; unpubl. observ.]. The reduction or elimination of the sampling bias against these small cells has begun to provide a more complete view of the circuit.

Functional and Evolutionary Relationship to Tuberous Processing in the Torus

The main result of this study is that the classes of ampullary neurons described above are similar to classes of tuberous neurons described in previous reports. The similarities include the frequency filtering profiles, shape of intracellular psp, and anatomy. For example, low-pass tuberous and ampullary neurons respond best to beat rates and sinusoidal frequencies, respectively, below 5 Hz; the smooth, stimulus-shaped intracellular responses and spiny dendrites are also similar [compare fig. 3 and 5 of Rose and Call, 1993, with fig. 1A, D]. The tuberous neuron shown in figure 2 of Rose et al. [1994] is similar to the high-pass neurons that have psp which roughly follow the shape of the stimulus and the band-pass neuron shown in figure 1E. The high-pass tuberous neurons shown in figures 7 and 8 of Rose and Call [1993] are remarkably similar to the neuron shown in figure 1F. The neurons where the psp width did not vary with stimulus frequency (fig. 3) do not have tuberous counterparts in the published literature. However, during the course of this experiment, we recorded from two tuberous neurons with similar voltage sensitive psp. The absence of these neurons in the literature may be a result of a sampling bias against small neurons imposed by sharp electrodes.

The physiological and anatomical similarities of the toral neurons indicate that the intrinsic circuitry of, and inputs to, the torus for both ampullary and tuberous information are also similar. A feature of the electroreceptive periphery of both the ampullary and tuberous systems is that the receptors are broadly tuned. At least until the level of the torus, there are no independent frequency channels within each of these systems. Electrosensory frequency informa-

tion in the torus, therefore, is derived from the afferent temporal codes. This stands in contrast to the auditory system of vertebrates, where frequency information is represented across separate channels originating from systematic differences in frequency selectivity at the periphery. These frequency channels are preserved and sharpened in the ascending auditory system [see Pollack, 1992; Suga, 1984].

The ampullary neurons described in this report respond to particular frequency ranges. These selectivities are generated from differences in processing of the afferent temporal code, not from the differences in the frequency selectivities of the afferents. Similarly, sensitivity to particular beat rates by tuberous neurons in the torus [Partridge et al., 1981] are also generated through differential processing of afferent temporal codes [for review see Heiligenberg, 1991]. The temporal codes of ampullary and tuberous afferents to the torus cover the same range of frequencies, from 1–30 Hz, and temporal filtering of both ampullary and tuberous codes within the torus are similar. These similarities are consistent with the hypothesis that the tuberous circuitry evolved as a duplication or elaboration of the 'older' ampullary circuitry.

The behavioral roles of the filtering properties of ampullary information in the torus are not known. Ampullary electroreceptors are involved in the detection of prey and possibly of predators [Himstedt et al., 1982; Kalmijn, 1982] and are involved in detecting interruption of the EOD during aggressive interactions with conspecifics and in courtship [Metzner and Heiligenberg, 1991; Hagedorn and Heiligenberg, 1985]. Similarly, the role of the tuberous filtering properties is also not well known. Certainly low-pass tuberous neurons contribute to the detection of the behavioral conditions that elicit JARs. However, such neurons may have more generalized functions, as moving stimuli can generate modulations at the same frequencies that elicit JARs [Rose et al., 1987]. Of particular interest, *Sternopygus*, the only wave-type genus of electric fish that does not have a JAR [Bullock et al., 1975], has tuberous neurons in the torus that have low- and band-pass filtering properties [Rose et al., 1987]. Also, neurons that combine phase and amplitude information to detect the direction of rotation in the amplitude-phase plane are present in *Sternopygus* [Rose et al., 1987]. These combination-sensitive neurons are seemingly an adaptation for the control of the JAR, but it is likely, since *Sternopygus* does not have a JAR, that these neurons also function in other behaviors (e.g. electrolocation). Another compelling possibility is that the functional organization of this circuitry reflects the evolutionary history of the ampullary and tuberous systems. Identification and characterization of the various behaviors

that require these circuits in both the ampullary and tuberos systems are necessary for understanding their functions and evolution. Alternatively, temporal filtering in the ampullary and tuberos systems may have evolved in parallel. This could be further tested by an outgroup comparison (i.e., with siluriforms).

Relationship of Morphology and Physiology

What is the contribution of spines to the shape and amplitude of psp recorded at the soma? Spines might represent high input impedance environments for synaptic inputs; conductance and therefore axial current flow might be limited primarily by the spine stem, by the synaptic ion channels associated with the receptor, or by both. For a maximum synaptic conductance of 1 nS, spine stems less than 2 μm in length and 0.05 μm in diameter are only expected to reduce by <30% the transfer of charge from the spine head to parent dendrite [Harris et al., 1992]; these dimensions are representative of the longest, thinnest spines seen on CA1 hippocampal pyramidal neurons. The precise dimensions of dendritic spines on low-pass toral neurons remains to be determined; many spines, however, are greater than 2 μm in length. Calculation of the extent to which the axial resistance of spine stems limits transfer of charge to the parent dendrite requires an estimate of the synaptic conductance at the spine head. Simulation results suggest that, if all spines have inputs, the average G_{max} for each input may be as low as 0.3 nS. Therefore for a spine with a stem of 2 μm in length and 0.5 μm in width, approximately 30% of the resistance to current flow from the synapse to the dendrite would be attributable to the stem; this figure may be as high as 60% for spines with stems of 4 μm in length. Presently, we can only conclude that the individual synaptic events occurring at the spines contribute little to the depolarization of the soma of low-pass neurons.

Neurons with high spine densities should therefore have smooth somatic psp that reflect the low-pass filtered sum of input conductances onto the dendrites. In contrast, neurons with few spines should have a greater percentage of axial synapses, resulting in larger axial currents, and smaller capacitance due to the reduced membrane surface area. As a result, few, or perhaps even single, synaptic conductances may result in detectable psp at the soma. We found that the psp of the very spiny neurons were smooth and sinusoidally shaped at low frequency stimulation. Neurons with few or no spines had a greater variety of psp shapes, but none had smooth, sinusoidal stimulus-related psp. All aspiny neurons had synaptic 'noise' that was visible at the soma; these psp may have originated from single input conductances. Thus, the data support the hypothesis that

spines may contribute to reducing synaptic noise at the soma and increase temporal summation of the neuron.

Similarly, all spiny ampullary neurons had low- or band-pass filtering characteristics, and all of the high-pass neurons were aspiny. What is the relationship of spine density to temporal filtering? In a previous report, spine density was shown to be positively correlated with temporal filtering [Rose and Call, 1993]. These findings strengthen the hypothesis of a functional link between dendritic spines and low-pass temporal filtering. Nevertheless, the answer to this question requires that we differentiate between the role of cellular properties versus filtering that is a result of the network properties of the neuron. One of the band-pass neurons, for instance, was morphologically indistinguishable from the low-pass neurons. In this case it is likely that the differences in frequency-filtering result from differences in the network properties of this neuron. Specifically, the adaptation at low frequencies may result from the negative feedback projection of Nucleus praeminentialis onto the electrosensory lateral line [Bastian, 1986, 1995].

Our data suggest that low- and band-pass neurons (spiny neurons) integrate synaptic inputs according to the passive electrical properties of the cell and fire at a set threshold. In contrast, four of the high-pass neurons (aspiny neurons) showed clear evidence for active conductance(s) that increased gain at higher frequency stimulation. Active conductances may be a common mechanism to increase gain at high stimulation frequencies. In the visual system of flies, low-pass 'CH' neurons follow temporal frequencies of visual moving stimuli of up to about 10 Hz and high-pass 'HS' neurons follow stimuli up to 40 Hz. Voltage-clamp experiments demonstrate that the high-pass neurons increase gain at high frequency stimulation using a fast, voltage-gated sodium current that is not present in the low-pass neurons [Borst, 1995]. Neurons in the medial vestibular nucleus of chicks (*Gallus domesticus*) also appear to use active conductances to increase gain at high frequency stimulation [du Lac and Lisberger, 1995]. When neurons were hyperpolarized below their firing threshold and sinusoidal current injected, they showed low-pass filtering with corner frequencies of approximately 6 Hz. However, in the absence of hyperpolarizing current, these neurons had broadband or slightly high-pass frequency responses. The differences between the subthreshold membrane potential and the activity at normal resting potentials reflect the action of active membrane conductances that increase gain at high frequency stimulation to overcome the passive low-pass filtering membrane characteristics [du Lac and Lisberger, 1995].

Acknowledgments

We thank Candace Hisatake for histological assistance and presentation of anatomical data. Supported by NSF grants IBN-9421039, IBN-91156789, and NIH NRSA fellowship 1 F32 NS09779-01.

References

- Bastian, J. (1986) Electrolocation: behavior anatomy, and physiology. In *Electroreception* (ed. by T.H. Bullock and W. Heiligenberg), John Wiley and Sons, New York, pp. 577-612.
- Bastian, J. (1995) Electrolocation. In *Handbook of Brain Theory and Neural Networks* (ed. by M.E. Arbib), MIT Press, Cambridge, pp. 352-356.
- Bodznick, D., and R.G. Northcutt (1981) Electroreception in lampreys: evidence that the earliest vertebrates were electroreceptive. *Science*, *212*: 465-467.
- Borst, A. (1995) How do nerve cells compute? Dendritic integration in fly visual interneurons. *Proceedings of the Fourth International Congress of Neuroethology*, p. 95.
- Bullock, T.H., and W. Heiligenberg, eds. (1986) *Electroreception*. John Wiley and Sons, New York.
- Bullock, T.H., R.H. Hamstra, and H. Scheich (1972) The jamming avoidance response of high frequency electric fish. I. General features. *J. Comp. Physiol.*, *77*: 1-22.
- Bullock, T.H., K. Behrend, and W. Heiligenberg (1975) Comparison of the jamming avoidance response in gymnotoid and gymnarichid electric fish: a case for convergent evolution of behavior and its sensory basis. *J. Comp. Physiol.*, *103*: 97-121.
- Carr, C.E., and L. Maler (1985) A Golgi study of the cell types of the dorsal torus semicircularis of the electric fish *Eigenmannia*: functional and morphological diversity in the midbrain. *J. Comp. Neurol.*, *235*: 207-240.
- du Lac, S., and S.G. Lisberger (1995) Cellular processing of temporal information in medial vestibular nucleus neurons. *J. Neurosci.*, *15*: 8000-8010.
- Hagedorn, M., and W. Heiligenberg (1985) Court and spark: electric signals in the courtship and mating of gymnotoid electric fish. *Anim. Behav.*, *33*: 254-265.
- Harris, K.M., F.E. Jensen, and B. Tsao (1992) Three-dimensional structure of dendritic spines and synapses in rat hippocampus (CA1) at postnatal day 15 and adult ages: implications for the maturation of synaptic physiology and long-term potentiation. *J. Neurosci.*, *12*: 2685-2705.
- Heiligenberg, W. (1973) Electrolocation of objects in the electric fish *Eigenmannia* (Rhamphichthyida, Gymnotoidei). *J. Comp. Physiol.*, *87*: 137-164.
- Heiligenberg, W. (1991) *Neural Nets in Electric Fish*. MIT Press, Cambridge.
- Heiligenberg, W., and G.J. Rose (1985) Phase and amplitude computations in the midbrain of an electric fish: intracellular studies of neurons participating in the jamming avoidance response of *Eigenmannia*. *J. Neurosci.*, *2*: 515-531.
- Himstedt, W., J. Kopp, and W. Schmidt (1982) Electroreception guides feeding behavior in amphibians. *Naturwissenschaften*, *69*: 552.
- Hopkins, C.D. (1976) Stimulus filtering and electroreception: tuberous electroreceptors in three species of gymnotoid fish. *J. Comp. Physiol.*, *111*: 171-207.
- Hopkins, C.D. (1983) Functions and mechanisms in electroreception. In *Fish Neurobiology*, Vol. 1: Brain Stem and Sense Organs (ed. by R.G. Northcutt and R.E. Davis), Univ. of Michigan Press, Ann Arbor, pp. 215-259.
- Kalmijn, A.J. (1982) Electric and magnetic field detection in elasmobranch fishes. *Science*, *218*: 916-918.
- Matsubara, J.A., and W. Heiligenberg (1978) How well do electric fish electrolocate under jamming? *J. Comp. Physiol.*, *125*: 285-290.
- Metzner, W., and W. Heiligenberg (1991) The coding of signals in the electric communication of the gymnotiform fish *Eigenmannia* from electroreceptors to neurons in the torus semicircularis of the midbrain. *J. Comp. Physiol. A*, *169*: 135-150.
- Partridge, B.L., W. Heiligenberg, and J. Matsubara (1981) The neural basis of a sensory filter in the jamming avoidance response: no grandmother cells in sight. *J. Comp. Physiol.*, *145*: 153-168.
- Pollack, G.D. (1992) Adaptations of basic structures and mechanisms in the cochlea and central auditory pathway of the mustache bat. In *The Evolutionary Biology of Hearing* (ed. by D.B. Webster, R.R. Fay, and A.N. Popper), Springer-Verlag, New York, pp. 751-778.
- Rose, G.J., and W. Heiligenberg (1986) Neural coding of difference frequencies in the midbrain of the electric fish *Eigenmannia*: reading the sense of rotation in an amplitude-phase plane. *J. Comp. Physiol. A*, *158*: 613-624.
- Rose, G.J., C.H. Keller, and W. Heiligenberg (1987) 'Ancestral' neural mechanisms of electrolocation suggest a substrate for the evolution of the jamming avoidance response. *J. Comp. Physiol.*, *160*: 491-500.
- Rose, G.J., and S.J. Call (1992) Evidence for the role of dendritic spines in the temporal filtering properties of neurons: the decoding problem and beyond. *Proc. Natl. Acad. Sci. USA*, *89*: 9662-9665.
- Rose, G.J., and S.J. Call (1993) Temporal filtering properties of neurons in the midbrain of an electric fish: implications for the function of dendritic spines. *J. Neurosci.*, *13*: 1178-1189.
- Rose, G.J., N. Etter, and T.B. Alder (1994) Responses of electrosensory neurons in the torus semicircularis of *Eigenmannia* to complex beat stimuli: testing hypotheses of temporal filtering. *J. Comp. Physiol. A*, *175*: 467-474.
- Rose, G.J., and E.S. Fortune (1996) New techniques for making whole-cell recordings from CNS neurons in vivo. *Neurosci. Res.*, in press.
- Roth, A., and P. Schlegel (1988) Behavioral evidence and supporting electrophysiological observations for electroreception in the blind cave salamander *proteus-anguinus* urodela. *Brain Behav. Evol.*, *32*: 277-280.
- Suga, N. (1984) The extent to which biosonar information is represented in the bat auditory cortex. In *Dynamic Aspects of Neocortical Function* (ed. by G.M. Edelman, W.E. Gall, and W.M. Cowan), John Wiley and Sons, New York, p. 315.
- Thomson, K.S. (1977) On the individual history of cosine and possible electroreceptive function of the pore-canal system of fossil fishes. In *Problems in Vertebrate Evolution* (ed. by S.M. Andrews, R.S. Miles, and A.D. Walker), Academic, New York, pp. 247-272.
- Zakon, H.H. (1986) The electroreceptive periphery. In *Electroreception* (ed. by T.H. Bullock and W. Heiligenberg), John Wiley and Sons, New York, pp. 103-156.